Supplemental Information

Structure and dynamics of an electrolyte confined in charged nanopores

Pierre-André Cazade,[1,2] Remco Hartkamp,[1,3] and Benoit Coasne[1,3,4,*]

[1] *Institut Charles Gerhardt Montpellier, UMR 5253 CNRS, Université Montpellier, ENSCM, 8 rue de l'Ecole Normale, 34096 Montpellier Cedex 05, France*

[2] *Institute of Physical Chemistry, Basel University, Klingelbergstrasse 80, 4056 Basel, Switzerland*

[3] *MultiScale Materials Science for Energy and Environment, CNRS-MIT (UMI 3466), Massachusetts Institute of Technology, 77 Massachusetts Avenue, Cambridge 02319, MA, USA*

[4] *Department of Civil and Environmental Engineering, Massachusetts Institute of Technology, 77 Massachusetts Avenue, Cambridge 02319, MA, USA*

This document first treats the terms in the modified Poisson-Boltzmann equation relevant for our purpose and then a few words are devotes to solving the equation numerically. As described in the paper, the equation of interest is the Poisson-Boltzmann equation in a cylindrical geometry, supplemented with terms that account for the position-dependent polarization of the water and an external potential to account for various interactions that are not included in the classical theory.

I. THEORY

The electrostatic potential $V(r)$ is related to the charge density ρ_e by the following equation:

$$\frac{1}{r}\frac{d}{dr}\left(-\epsilon_0 r\frac{dV(r)}{dr}\right)+\frac{dP(r)}{dr}=\rho_e(r), \tag{1}$$

where ϵ_0 is the dielectric permittivity of a vacuum, $P(r)$ is the position-dependent polarization of the water[1] and the charge density on the right hand side follows from the density distributions of the ionic species $\rho_e(r)=e(\rho_+(r)-\rho_-(r))$, which in turn is a function of the electrostatic potential. In order to solve Eq. (1), we need to quantify the polarization term, relate the density distribution of the ionic species to the electrostatic potential and define boundary conditions of the differential equation.

The position-dependent polarization can be approximated in terms of the potential, according to the step polarization (SP) model:

$$\frac{dP(r)}{dr}=\begin{cases}0, & \text{if} \quad r<r_0,\\ -\epsilon_0(\epsilon_w-1)\frac{d^2V(r)}{dr^2}, & \text{if} \quad r\geq r_0,\end{cases} \tag{2}$$

where ϵ_w is the dielectric permittivity constant of water ($\epsilon_w=78$ for the water model that we use) and r_0 is the position of the first peak in the oxygen profile. Alternatively, the position-dependent polarization can be approximated in terms of the oxygen and hydrogen density profiles that are

measured from the molecular dynamics simulations, following the full polarization (FP) model:

$$\frac{dP(r)}{dr} = -\left(q_O \rho_O(r) + q_H \rho_H(r)\right). \tag{3}$$

The charges for the POL3 water model[2] are $q_O = -0.730$e and $q_H = 0.365$e. Both models have been applied in the paper.

We make a mean-field approximation for the density distribution of monovalent ionic species in a thermodynamic equilibrium:

$$\rho_\pm(r) = \rho_0 \exp\left(-\beta(\pm eV(r) + U_\pm^{ext}(r))\right), \tag{4}$$

where $\beta = 1/k_\mathrm{B}T$, ρ_0 is the bulk ion density, e is the elementary charge and $U_\pm^{ext}(r)$ is the external potential profile for the cation (+) and the anion (−). Using Eq. (4) we can express the charge density profile as:

$$\rho_e(r) = e\rho_0 \left(\exp\left(-\beta(eV(r) + U_+^{ext}(r))\right) - \exp\left(\beta(eV(r) - U_-^{ext}(r))\right)\right). \tag{5}$$

Combining this result with Eqs. (1) and (3) gives us the differential equation to solve, with the external potentials and the boundary conditions to specify next. The external potentials for the cation and anion species consist of the sum of three contributions: $U_\pm^{ext} = U^{im} + U_\pm^{LJ} + U_\pm^{hyd}$. Each of these terms will be briefly discussed in the following.

The image charge potential describes the interaction between ions and a dielectric interface, which is located at a distance r_0 from the wall.[3,4] The image potential is given by:

$$U^{im}(r) = \left(\frac{\epsilon_w - 1}{\epsilon_w + 1}\right) \frac{e^2 \exp(-2(r - r_0)/\lambda)}{16\pi\epsilon_0\epsilon_w(r - r_0)}, \tag{6}$$

where λ is the Debye screening length, given by:

$$\lambda = \sqrt{\frac{\epsilon_0\epsilon_w}{2\beta e^2 \rho_0^2}}. \tag{7}$$

For our systems, the Debye length is $\lambda = 2.24$ Å.

The ion-wall Lennard-Jones interaction $U_\pm^{LJ}$ is a term that accounts for the Lennard-Jones interactions between an ion and the wall. This term depends strongly on the configuration of the wall. We calculated this term for our system by placing an ion at different positions in the carbon nanotube and for each position summing all the interactions between the ion and the wall atoms. The sampling can be done either by placing the ion at random positions in the channel and using a histogram method, or by systematically scanning a part of the domain that is sufficiently large to account for the structure of the wall (e.g., the hexagonal carbon lattice). We have applied the latter approach in order to exploit the highly regular structure of the carbon. After averaging the collected information over the angular direction and the tube direction one obtains as a function of the radial position only.

The hydrophobic solvation energy term describes the solvation energy associated with the removal of ions from the water. The expression for this term is given by:

$$U_\pm^{hyd}(r) = C_0 \left(v_\pm^{imm}(r) - v_\pm^{ion}\right), \tag{8}$$

where C_0 is the solvation free energy per unit volume, $v_{\pm}^{ion}$ is the total volume of and ion with a solvent-excluded diameter of $\sigma_{\pm}$, and $v_{\pm}^{imm}(r) = \pi(3/2\sigma_{\pm}r_{\pm}^2 - r_{\pm}^3)/3$ for $0 \leq r_{\pm} \leq \sigma_{\pm}$, where $r_{\pm} = r - r_0 + \sigma_{\pm}/2$.

Figure S1 shows the contributing terms discussed above as well as the total external potential for the cation (+) and the anion (−). As expected, the location of the energy well for the cation is closer to the negatively charged wall (located at $r = 15$ Å) than that of the anion. Note that the calculated profiles depend on the configuration of the wall as well as on the material of the wall and the ions. However, no electrostatic effects are included in the external potential, since these are already fully accounted for by the electrostatic potential $V(r)$.

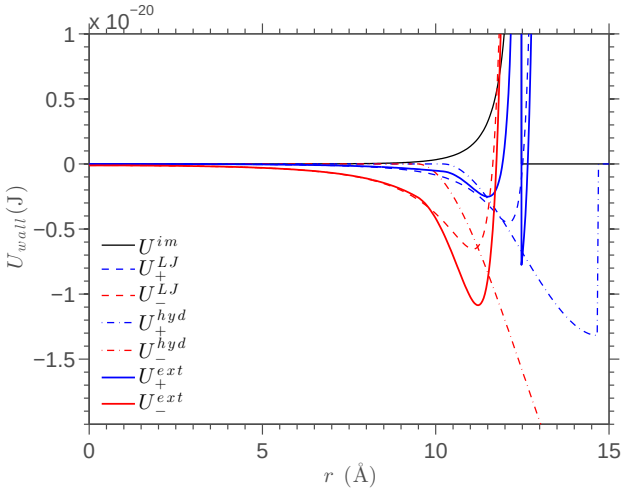

FIG. S1: (color online) External potential between an ionic particle and the carbon nanotube.

Many studies have been devoted to calculating the potential of mean force (PMF)[5,6] directly from molecular simulations as an alternative to the approach described above. The PMF calculations deviate from our approach in the sense that simulation data of the ionic species is used in the calculation of the mean force. This is inconsistent with our objective, since we try to predict the distribution of the ionic species, rather than using it as input. However, a comparison between a calculated PMF and our theoretical treatment can be used to confirm or optimize the terms in the external potential. Such a fine-tuning of the external potential is not pursued here since our simulation parameters do not correspond to a regime in which an accurate quantitative prediction can be made with the MPB equation.

II. SOLVING THE EQUATION

The Poisson-Boltzmann equation can only be solved analytically in a few special cases, e.g., with certain boundary conditions and by making assumptions to simplify the equation. The modified Poisson-Boltzmann problem considered here needs to be solved numerically. We start with an initial guess for the electrostatic potential and use a standard finite difference technique to approximate its gradients. We then use an iterative method[7] and perform several hundred iterations until the

solution has relaxed.

We solve the differential equation using Neumann boundary conditions at $r = 0$

$$\left.\frac{dV(r)}{dr}\right|_{r=0} = 0, \tag{9}$$

and at the wall $r = r_{wall} = 15$ Å

$$\left.\frac{dV(r)}{dr}\right|_{r=r_{wall}} = -\frac{\sigma_S}{\epsilon_0 \epsilon_w}, \tag{10}$$

where σ_S is the surface charge density. The first condition is required due to the symmetry of the system with respect to its center, whereas the second boundary condition is related to an integral of the charge density in the system. The boundary conditions are independent of the polarization term, since the integral over the polarization is zero.

III. STRUCTURE OF THE CONFINED ELECTROLYTE

Figure S2 shows the profiles of every species of the confined electrolyte in the four nanotubes considered. The maximum density of the oxygen falls outside of the graphs in order to display the data such that the ion distribution profiles are visible, as well as the locations of peaks and troughs.

IV. CORRECTION FINITE ION SIZE

Close to a charged surface, a dense layer of counterions forms as seen in the results above. The standard Poisson-Boltzmann equation is not able to predict layering in the concentration profile. This is due to the fact that Poisson-Boltzmann is a mean-field approach which does not include ion-ion correlations and does not take into account the heterogeneity of the solvent (density oscillations close to the pore surface). The ion concentration predicted using Poisson-Boltzmann in the double electrical layer depends on the bulk concentration and on the the surface charge density. When the surface charge and the ion concentration are large, the predicted ion density can exceed that of close packed ions by multiple orders of magnitude. This is a consequence of the fact that ions are treated as point charges in the Poisson-Boltzmann equation, rather than accounting for steric effects due to their finite size.[8] The same is true for the modified Poisson-Boltzmann equation that we have solved in the paper. We have accounted for the fact that the dielectric constant of the solvent is not homogeneous and we added an external potential term to account for various interaction forces. However, our modified equation does not take precautions to limit the maximum ion concentration.

There have been many attempts over the years to include corrections to the Poisson-Boltzmann equution to account for ions sizes. Many of these studies derived a correction term using density functional theory (DFT)[9,10] or variational methods[11–13] As mentioned in Section 3.1.2, DFT and PB both suffer from limitations in their ability to predict phenomena that occur on the molecular

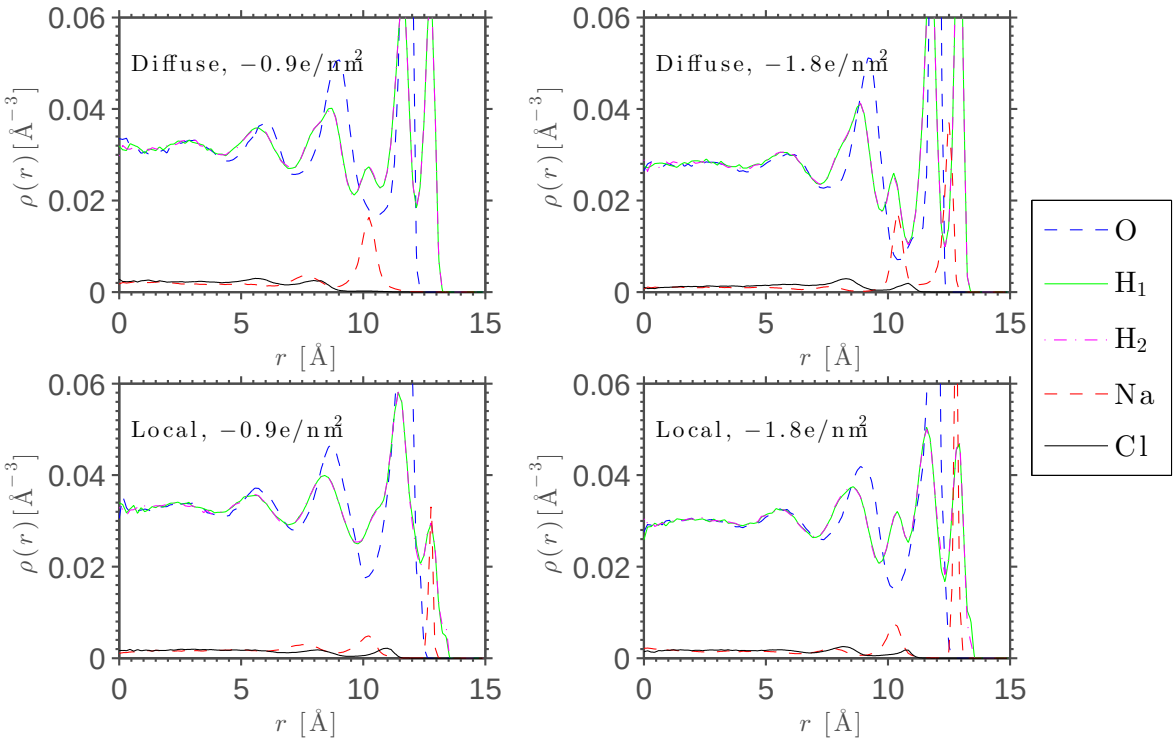

FIG. S2: (color online) Density profiles for each of the atom types present in the aqueous electrolyte solution: O (blue dashed line), H1 (green full line), H2 (magenta dash-dotted line), Na (red dashed line), and Cl (black full line). The figure shows two different surface charge strengths (-0.9 e/nm^2 on the left and -1.8 e/nm^2 on the right) and two different distributions of the surface charge (diffuse on top and local on bottom).

scale. Our intention here is not to overcome such challenges. We merely try to see how reasonably simple models are able to reproduce the results of our more sophisticated simulations. We add the simplest correction to account for the finite ion size and show its influence on the predicted ion concentration profile. We follow the pioneering work of Bikerman[14] who suggested the following corrected charge distribution to account for the finite volume fraction taken up by the ions:

$$\rho_{\pm}(r) = \frac{\rho_0 \exp\left(\mp \beta e V(r)\right)}{1 + \frac{\rho_0}{\rho_+^{max}}\left(\exp(-\beta e V(r)) - 1\right) + \frac{\rho_0}{\rho_-^{max}}\left(\exp(\beta e V(r)) - 1\right)}, \tag{11}$$

where the maximum (closely packed) cation and anion concentration, ρ_+^{max} and ρ_-^{max}, depends on the volume of the ions, which is not uniquely defined. We have chosen to use the radius of the hydration shell around sodium and chloride ions in a bulk solution ($r = 0.32$ nm for sodium and $r = 0.38$ nm for chloride, data not shown here), these radii are larger than the Lennard-Jones radius of the ions so that the influence of the correction term is expected to be larger. The correction term in Eq. (11) was presented in 1942 in a paper that later got forgotten about. Subsequently, it was independently introduced by other authors as discussed in Ref. 15.

We combine the correction term shown in Eq. 11 with the full polarization method as presented above, including the addition of the external energy term added to the Boltzmann distribution. Figure S3 shows the full polarization model (FP) as presented above, with and without the steric

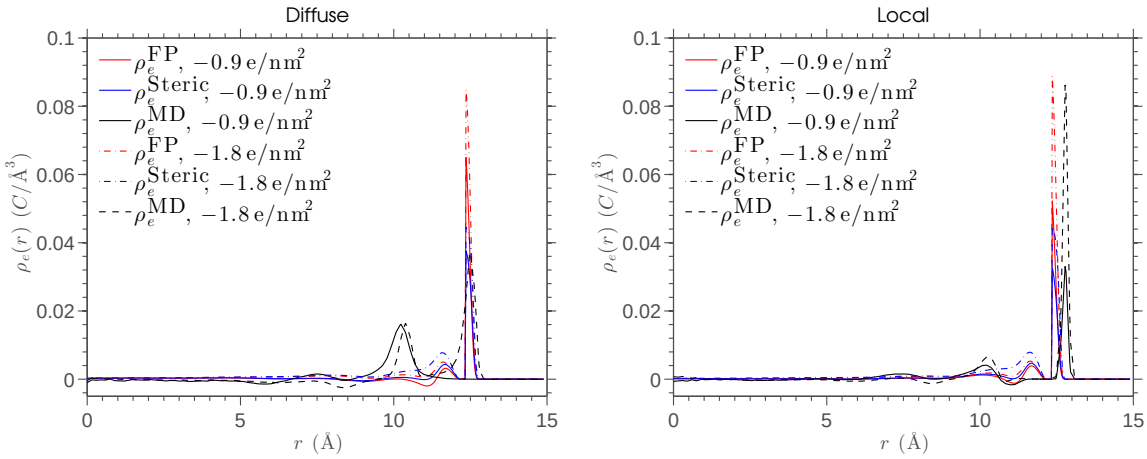

(a) (b)

FIG. S3: The full polarisation model (FP) with and without the steric correction term. The MD data is shown for comparison. (a) shows the case with the diffuse surface charge distribution, whereas (b) shows the case in which the surface charge is distributed over a subset of the atoms of the carbon nanotube.

correction term. The effect of the correction term on the maximum ion concentration is visible in the magnitude of the maximum charge density. On the other hand, the location of the peak has remained unchanged. Note that the concentration profiles in Figure S2 imply that the dense layer of cations is not surrounded by water molecules. Thus, the radii that we use in our correction term lead to a maximum allowed ion concentration that is smaller than that which would be possible in the simulation, so that we might be slightly overcorrecting the shortcoming of the traditional Poisson-Boltzmann equation. A more accurate quantitative comparison between the molecular dynamics data and the a modified Poisson-Boltzmann treatment would require a detailed study of the correction terms and corresponding parameter values appropriate for the simulation system.

References

* Electronic address: benoit.coasne@enscm.fr

[1] J. D. Jackson, *Classical electrodynamics*, 3rd ed. (John Wiley and Sons, New York, 1975) ISBN 9780471431329.

[2] J. W. Caldwell and P. A. Kollman, J. Phys. Chem., **99**, 6208 (1995).

[3] L. Onsager and N. N. T. Samaras, J. Chem. Phys., **2**, 528 (1934).

[4] B. Trninić-Radja, M. Sunjić, and Z. Lenac, Phys. Rev. B, **40**, 9600 (1989).

[5] B. Roux, Comp. Phys. Commun., **91**, 275 (1995).

[6] D. Horinek and R. R. Netz, Phys. Rev. Lett., **99**, 226104 (2007).

[7] P. Wesseling, *An Introduction to Multigrid Methods*, 2nd ed. (R.T. Edwards, 2004) ISBN 9781930217089.

[8] I. Borukhov, D. Andelman, and H. Orland, Phys. Rev. Lett., **79**, 435 (1997).

[9] D. Antypov, M. C. Barbosa, and C. Holm, Phys. Rev. E, **71**, 061106 (2005).

[10] J. Forsman, J. Phys. Chem. B, **108**, 9236 (2004).
[11] B. Eisenberg, Y. Hyon, and C. Liu, J. Chem. Phys., **133**, 104104 (2010).
[12] D. Fraenkel, Mol. Phys., **108**, 1435 (2010).
[13] G. Wei, Q. Zheng, Z. Chen, and K. Xia, SIAM Rev., **54**, 699 (2012).
[14] J. Bikerman, Philos. Mag., **33**, 384 (1942).
[15] M. Z. Bazant, M. S. Kilic, B. D. Storey, and A. Ajdari, Advances in Colloid and Interface Science, **152**, 48 (2009).